RESEARCH PAPER

Physical and Structural Characteristics of Gel-Derived Glasses Prepared via Different Drying Procedures

Sara Ahmadi[1,*], Bijan Eftekhari Yekta[2], Hossein Sarpoolaky[2], Alireza Aghaei[3]

* *s.ahmadi@standard.ac.ir*

[1] Construction and Minerals Research Group, Technology and Engineering Research Center, Standard Research institute, Alborz, Iran

[2] Ceramic Division, School of Materials and Metallurgy Engineering, Iran University of Science and Technology, Tehran, Iran.

[3] Ceramic Department, Materials and Energy Research Center (MERC), Alborz, Iran

Received: June 2021 **Revised: August 2021** **Accepted: September 2021**

DOI: 10.22068/ijmse.2297

Abstract: *The monolithic gels were prepared through different drying procedures including super critical, infrared wave lengths and traditional drying methods. Dense and transparent glasses with chemical composition of $66SiO_2$-$18B_2O_3$-$7Al_2O_3$-$6K_2O$ -3BaO (in wt.%) were obtained after controlled heat treatment of the dried porous xerogels at 950°C for 2 h in air atmosphere. The chemical bonding as well as different properties of the prepared gels and the relevant glasses were investigated by means of Fourier transform infrared spectroscopy (FTIR), Brunauer-Emmitt-Teller (BET) and UV-Vis spectrometer. The results indicates that different drying conditions affect the average pore size and the total pore volume of the studied gels. The mean pore size was found to be 8.7, 2.4 and 3.2 nm for super critical, IR radiation and slow drying in air respectively. The glass network structure was significantly changed by heat treatment temperature such that the B-O-Si bonds were formed only after 450°C. It was found that the gel dried under super critical condition was unable to reach to its full density under the sintering conditions adopted in this study.*

Keywords: *Sol-gel glass, Super- critical drying, IR drying, Sintering activation energy.*

1. INTRODUCTION

Recently, growing attention has been focused on preparation of the sol-gel derived glasses. This method is based on the two main steps including hydrolysis and subsequent condensation of the metal alkoxides or salts. Various factors involved in the described steps such as solution pH, H_2O/TEOS ratio, synthesis temperature and aging conditions have been the topic of a wide number of investigations [1-5].

It is worth mentioning that the drying procedures are highly significant to prepare crack free monolithic gel derived glasses. In this regard, super critical drying is an appreciate method to dry monolithic gels [6]. In this method, by elimination of the interfaces between the liquid and vapor phases, the driving force for gel shrinkage is reduced. Hence, the capillary pressure, which causes the cracks during drying, approaches to zero [6-10]. However, this drying technique has been limited due to its high cost and risk [11-13]. Therefore, it seems drying techniques at ambient pressure (subcritical drying) which form xerogel structures, are inevitable to obtain crack free gel derived glasses. Infrared radiation drying is one of the most useful drying methods with much higher drying rate rather than that of the air drying methods. Thanks to the high penetration of infrared rays, infrared radiation is converted to heat inside the body and leads to heating up all over the sample, homogeneously. By using infrared radiation drying, water evaporation takes place from both inside and outside of the specimen, simultaneously with accelerated drying rate [14, 15]; whereas in the ordinary drying techniques, the surface temperature is usually more than the inside.

The structure of dried gels is equivalent to that of the corresponding glasses [1, 16], but less condensed and containing excess free volume. Gel structural skeleton approaches to that of melt derived glasses, if only heated to higher temperatures. During structural transformation of gel to glass, particles welding results in progressive pore elimination by diffusion and viscose flow mechanisms. In the gel to glass transformation, the residual OH and OR groups are removed in the form of H_2O and ROH, which is accompanied by additional network polymerization and causes considerable weight

[DOI: 10.22068/ijmse.2297]

loss and shrinkage. Finally, when the temperature is high enough, rapid shrinkage and the collapse of large pores occur by viscose sintering [1].
In the present work, the effect of different drying methods on physical properties of the prepared gels and their relevant glasses has been investigated. The gel to glass transformation mechanism during heat treatment has been also discussed and characterized.

2. EXPERIMENTAL PROCEDURE

2.1. Materials and methods

A borosilicate glass with chemical composition of $66SiO_2$-$18B_2O_3$-$7Al_2O_3$-$6K_2O$ -3BaO (in wt. %) [17] was prepared from reagent grade chemicals of tetraethyl orthosilicate (TEOS, $(Si(OC_2H_5)_4)$, aluminum-sec-butoxide ($Al(OC_4H_9)_3$), trimethyl borate ($B(OCH_3)_3$), barium and potassium acetate (99.9 pure). To this purpose, a dilute solution of 1TEOS: 4ethanol (molar ratio) was hydrolyzed gradually by addition of 1 M HCl solution. The molar ratio of H_2O/Si was kept 4:1. After 2 h, the solution of Al-sec-butoxide in isopropanol alcohol (1:4 molar ratios) was added to it, slowly. The resulted solution was stirred until a transparent solid free solution was obtained. Then, trimethyl borate with stoichiometric amount of water was added to hydrolyze the aluminum and boron alkoxides. Finally, aqueous solution of barium acetate (1 M) and potassium acetate (2 M) were added. The final solution with an increased water content (2-3 times more than that of the stoichiometric amount required to fully hydrolyze the alkoxide) was stirred for 2 h to insure complete hydrolyzing of the alkoxides and homogenizing of the resulted sol. Then, it was casted into polypropylene tubes and covered with aluminum foil. Gelation occurred after 24 h at room temperature.
The wet gel was aged at 45°C for 10 days in an aging solution containing water, ethanol and propanol with similar composition to what was used for gel preparation. Afterward, the gels were dried through three different methods: i) slow drying at air atmosphere (AD), ii) drying above the critical point of CO_2 (32°C, 82 bar) after ethanol replacement by liquid CO2 (SCD), and iii) drying under infrared radiation (IRD).
In the first method, samples were dried at room temperature. In the second method, the wet gel was placed inside an autoclave and after replacement of pore liquid by liquid CO_2, heated above critical point of CO_2 (32°C, 82 bar). The autoclave was then cooled down and the gel removed at ambient pressure in accelerated drying condition. In the third method, an infrared lamp (power of 150 w) was used, whilst the chamber temperature was set on 60°C and the distance between lamp and sample was 10 cm. Finally, the dried samples were converted to glass by heat treatment at 950°C for 2 h at the heating rate of 1ºC/min. Fig. 1 shows the flow chart of the described procedures. Sintering activation energy was estimated in non-isothermal condition based on the Cheng equation [18]:

$$\mathrm{Ln}\,(\nu/T^2) = -E/RT_x \qquad (2\text{-}1)$$

Where ν, T_x, E and R refer to the heating rate, temperatures corresponding to a fixed degree of transformation, activation energy for sintering and gas constant, accordingly. By plotting the variation of Ln (ν/T^2) versus 1/T, the activation energy of sintering via viscose flow mechanism can be measured from the plot slope.

2.2. Characterization techniques

The specific surface area and pore size distribution of the dried gels were examined by Brunauer-Emmett-Teller method (BET, Belsorp II mini). Chemical bonding states of the sintered gels were monitored using Fourier transform infrared spectroscopy (FTIR, Perkinelmer spectrum 400). Bulk density and densification behavior of the specimens were calculated based on the Archimedes method after heat treatment at different temperatures in air atmosphere.
Hot stage microscope (Misura 2.1 expert system) was used to study the activation energy of the viscose flow of the glass powder at the heating rates of 10, 15, 20 and 25°C/min. Crystallization behavior was investigated by X-ray diffraction technique (XRD, D-500 Simence). UV-Vis spectrometer (PG instrument model T80) was used to study the transparency of the obtained glasses at the wavelength interval of 400-800 nm. Vickers micro-hardness (Buehler, VH 1202 series) was measured under load of a 100 g indenter for 15 s.

3. RESULT AND DISCUSSION

The non-uniform contraction in the drying process, due to the different velocities of evaporation of water, is the main reason for cracking in the ceramic products.

[DOI: 10.22068/ijmse.2297]

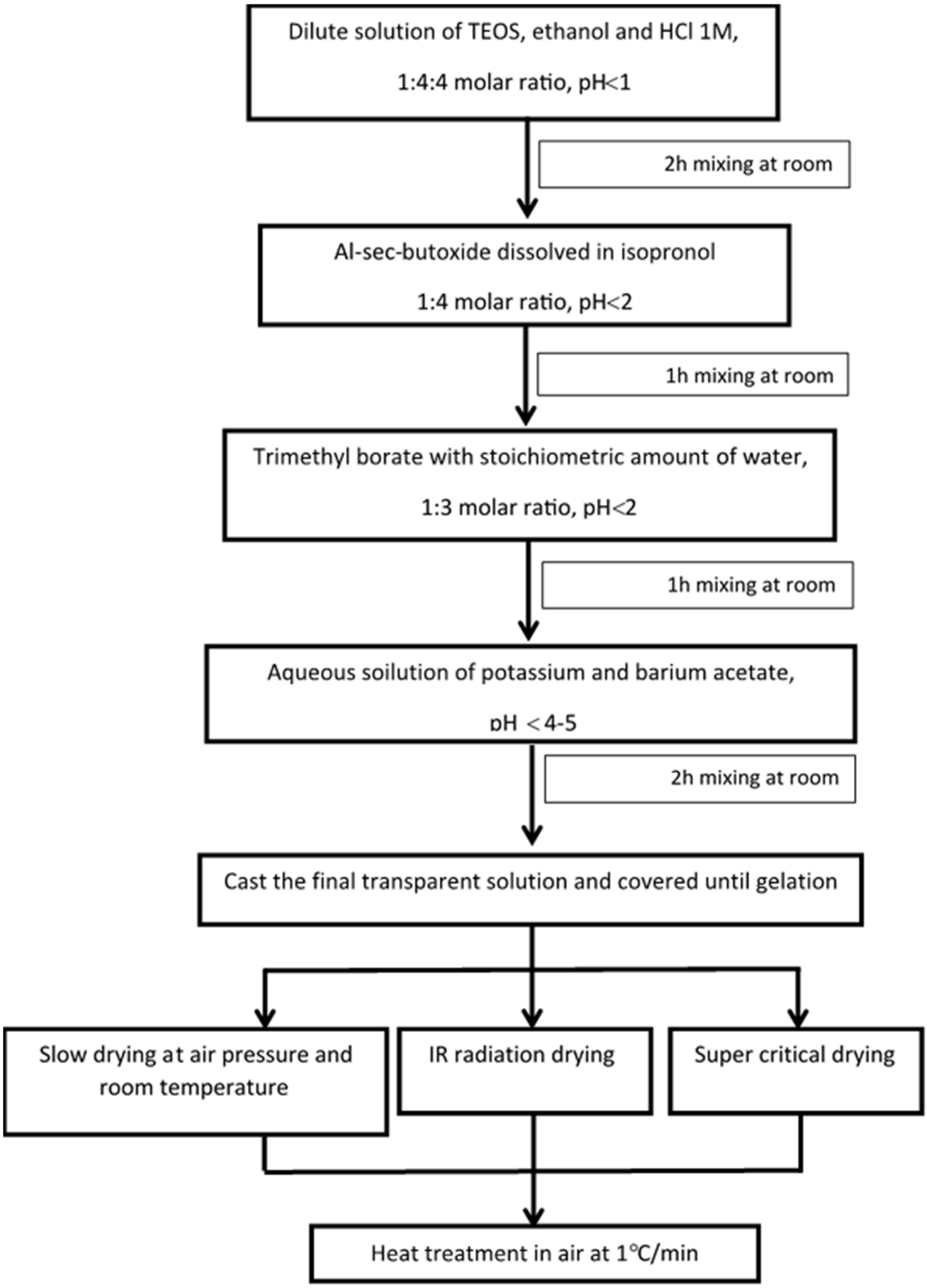

Fig. 1. Flow diagram of the chemical preparation procedures.

[DOI: 10.22068/ijmse.2297]

Because of the high volume of water and alcohol used in the sol-gel method and also the lower strength of gels in this method, the drying process in the sol-gel method is the most important step in the preparation of monolithic crack-free dried gels and has a special sensitivity.

The amount of shrinkage in the sample is proportional to the drying speed and the size of it. Therefore, the air drying process should be very slow to prevent cracking in the drying of gels prepared by sol-gel. In this research, this process took more than two months. Using the infrared drying process, this process is greatly shortened to about 10 hours. On the other hand, with the supercritical drying method, this process was much faster and took about 5 hours. Fig. 2 shows the monolithic samples which have been dried slowly at room temperature. As it can be observed the dried gel is adequately transparent and crack-free.

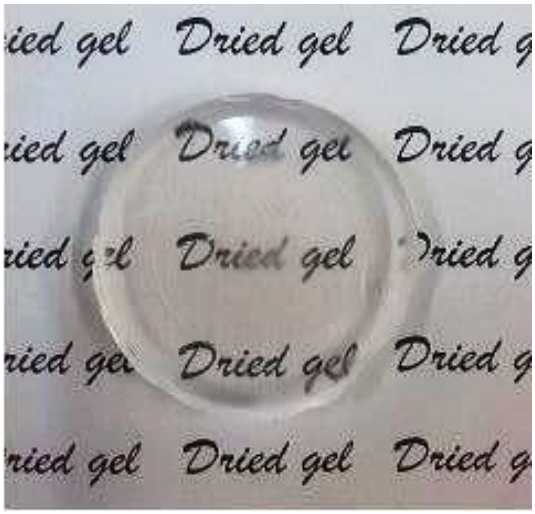

Fig. 2. Monolithic dried gels prepared after 2 month slow drying at room temperature (AD)

Fig. 3 shows the pore size distributions (BJH-plot) of the samples dried in the three different conditions. It can be realized that the samples display a symmetric pore size distribution.

Accordingly, the average pore size of the dried gels was changed differently in super critical or ambient pressure. Specific surface area, average pore size and total pore volume of the samples have been summarized in Table 1.

From Table 1, the average pore size and total pore volume are much higher in the SCD samples compared to the AD and IRD ones. It should be mentioned that during drying process, the AD and IRD dried samples experienced more linear shrinkage, i.e. 41.11% and 56.84%, respectively compared to the SCD sample with 6.2% linear shrinkage. This led to presence of smaller and less interconnected pores within AD and IRD dried specimens. Since in the super critical drying condition, there was no interface between the liquid and vapor phases and consequently there was no difference between solid-liquid and solid-vapor interfacial energies, the driving force for gel shrinkage was reduced; hence the capillary pressure was equaled to zero [12]. In the case of ambient pressure drying, the gel structure was continuously contracted until there was a liquid to be evaporated. This led to formation of small pore diameters compared to the SCD gels.

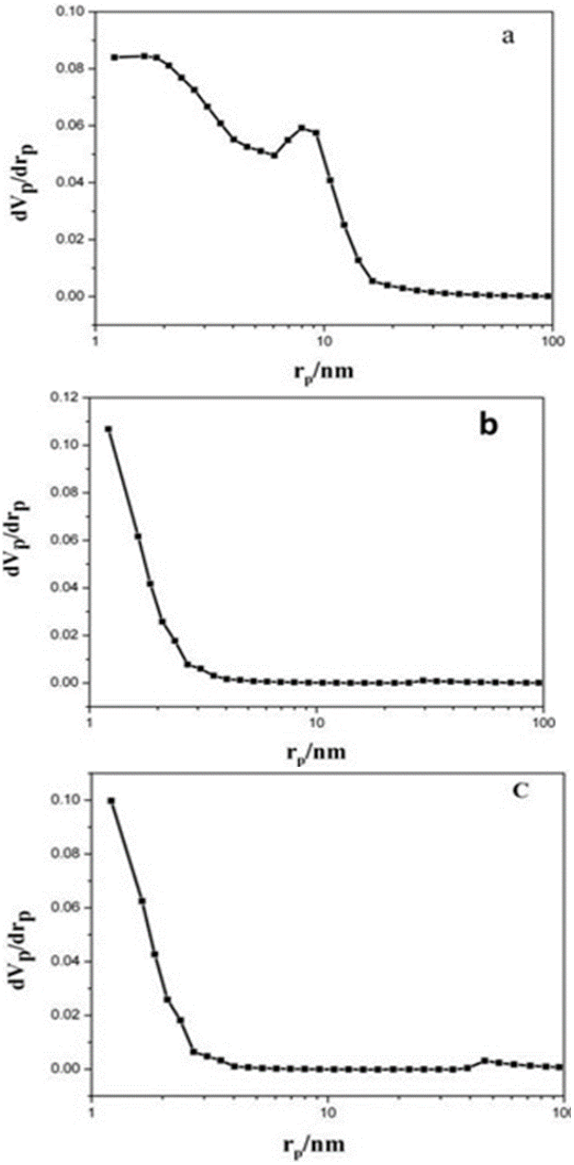

Fig. 3. The pore size distribution of the dried gel (a) SCD, (b) IRD and (c) AD.

[DOI: 10.22068/ijmse.2297]

Table 1. BET results of the SCD, IRD and AD dried specimens.

Drying condition	Specific surface area (m^2/g)	average pore size (nm)	Total pore volume (m^3/g)
SCD	348±1.2	8.73±0.38	0.759±0.08
IRD	465±1.5	2.43±0.33	0.283±0.05
AD	369±1.3	3.22±0.4	0.289±0.05

Fig. 4 shows the bulk density variation of the prepared gels dried under three different methods and heat treated in static air atmosphere. The bulk density variation of the AD and IRD dried glasses followed a similar trend and their bulk density was higher than that of the SCD dried glass. This behavior is attributed to the more linear shrinkage throughout the AD and IRD processes as mentioned, previously. The true density of the specimen heat treated at 950ºC for 2 h was 2.2000±0.0032 g/cm^3. Therefore, it can be deduced that the porous super critical dried aerogels cannot be completely densified even at temperatures above 1100°C. But, the ambient pressure dried samples can reach full densification at temperature interval of 900-950°C, thanks to contain initially smaller and lower pores than the SCD specimens. In other words, due to presence of initially larger and higher pores in the SCD specimen, the viscose flow process during heat treatment is not capable to remove all pores.

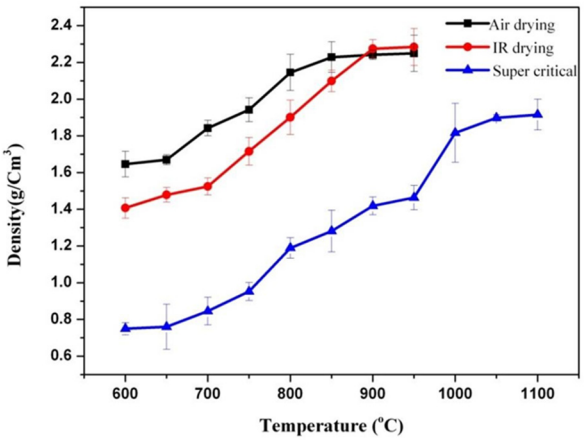

Fig. 4. Bulk density variation of gels versus firing temperature. Lines are shown as guides for the eyes.

The SEM micrograph of the SCD glass heat treated at 1100ºC for 2 h (shown in Fig. 5) is in conformity with this result. As can be observed, the microstructure is completely porous and contains abundant pores with dimension smaller than 25 µm.

Fig. 6 shows the XRD pattern of the SCD and AD specimens after heat treatment at 950 and 1100°C for 2 h. Since the examined glasses are still amorphous in this step, no specific peak lines of crystalline phases are evident in this figure.

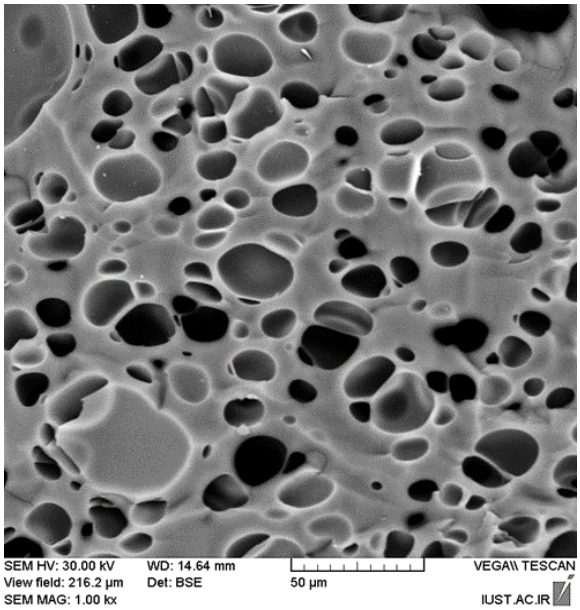

Fig. 5. SEM micrograph of the SCD glass after heat treatment at 1100ºC for 2 h.

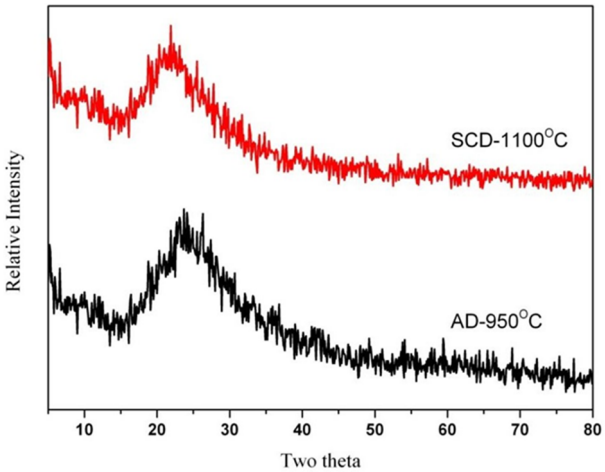

Fig. 6. XRD patterns of the AD and SCD glasses after heat treatment at 950 and 1100°C.

Fig. 7 depicts the variation of Vickers micro-hardness of the SCD and AD monolithic gels versus heat treatment temperature. The variations of micro-hardness and bulk density are almost

[DOI: 10.22068/ijmse.2297]

similar. Increase of glass micro-hardness with heat treatment temperature confirms the positive effect of sintering on the micro-hardness improvement. Moreover, the lower micro-hardness of SCD specimen is influenced by its foaming status

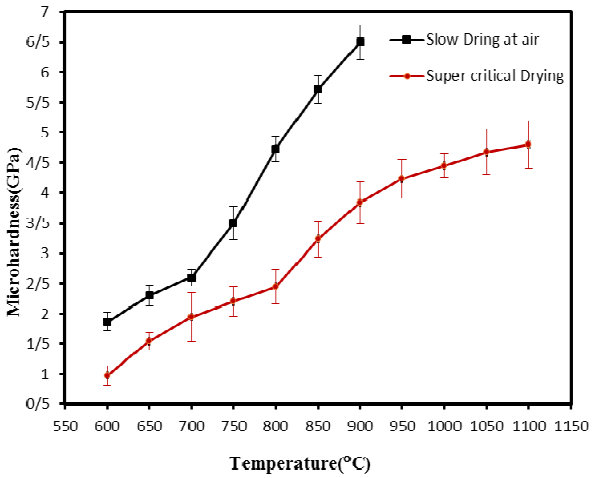

Fig. 7. Vickers micro-hardness of the AD and SCD gels versus heat treatment temperature. Lines are shown as guides for the eyes.

The transmission spectra of the specimens are shown in Fig. 8. It is evident that the AD and IRD glasses are completely transparent after sintering at 950°C for 2 h, whereas the SCD one shows lower transmission behavior even after sintering at 1100°C for 2 h, probably due to its low density and significant content of the remained pores.

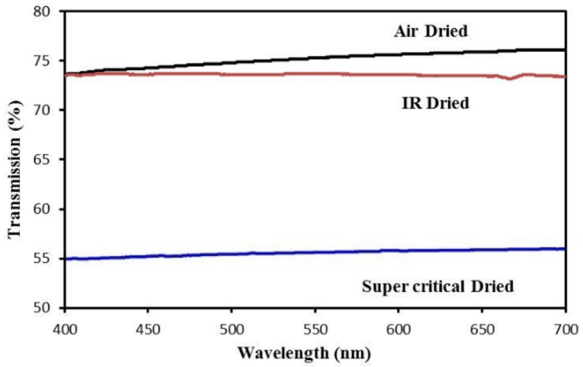

Fig. 8. UV–Vis transmittance spectra of the glasses dried under three different conditions as a function of wave length.

During gel to glass transition process, a simultaneous weight loss and shrinkage occurs in the specimens. Fig. 9 reveals the linear shrinkage and weight loss variation of the AD gel after heat treatment in static air atmosphere. Based on Fig.9, the gel to glass conversion process can be divided into three steps. The remarkable weight loss is observed in the first and second regions. Whilst, in the third region, the shrinkage increases notably, but the weight loss is negligible. It seems that elimination of physically absorbed H_2O and ROH is responsible for remarkable weight loss in the first region. However, concurrent shrinkage and weight loss in the second region can be attributed to the oxidation of organic compounds and removal of water from condensation reactions. A high shrinkage rate in the third step indicates that sintering happens in this temperature interval via viscous flow sintering [16].

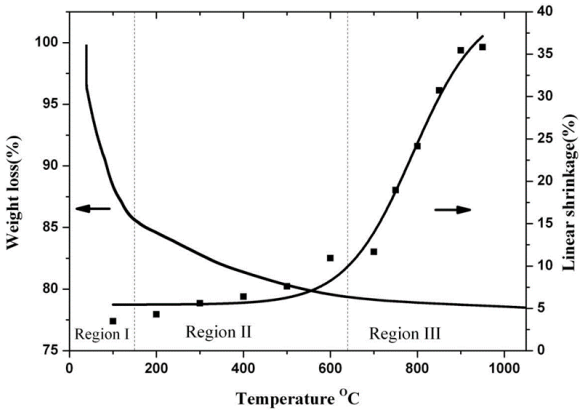

Fig. 9. Linear shrinkage and weight loss of the AD gel as a function of firing temperature. Lines are shown as guides for the eyes specimen during heat treatment at.

Gel to glass conversion during heat treatment was also examined by infrared spectroscopy. Fig.10 shows the FTIR spectra of the gels subjected to the different heating temperatures. The broad band located at 3700-3200 cm^{-1} and the peak at 1640 cm^{-1} are attributed to the physically adsorbed water [19]. The broad band gradually disappears with temperature increase due to the condensation reactions throughout gel to glass conversion. The peak located at 950 cm^{-1} can be corresponded to hydroxyl groups Si-OH in the specimens. The 1220 and 1080 cm^{-1} bands are assigned to stretching modes of Si-O, respectively. The band located at 800 cm^{-1} is related to the symmetric Si-O-Si stretching or vibration modes of the ring structures. The peak located at 460 cm^{-1} is due to the deformation of Si-O-Si bending mode [20, 21]. As shown in Fig. 10, the borosiloxane bonds indicated by 670 and 915 cm^{-1} vibration, are not detectable in the dried gel and form at approximately 600°C. The bands

[DOI: 10.22068/ijmse.2297]

located at 560 and 1415 cm^{-1} are referred to the B-O deformation and stretching modes in $B(OH)_3$, respectively. The intensity of these bands decreases by temperature increase. It is believed that boron mostly exists as B(OH) in the as-dried gel. Removal of water and alcohol during heat treatment leads to the formation of B-O-Si at 915 and 670 cm^{-1} bonds in expense of disappearing $B(OH)_3$ [22].

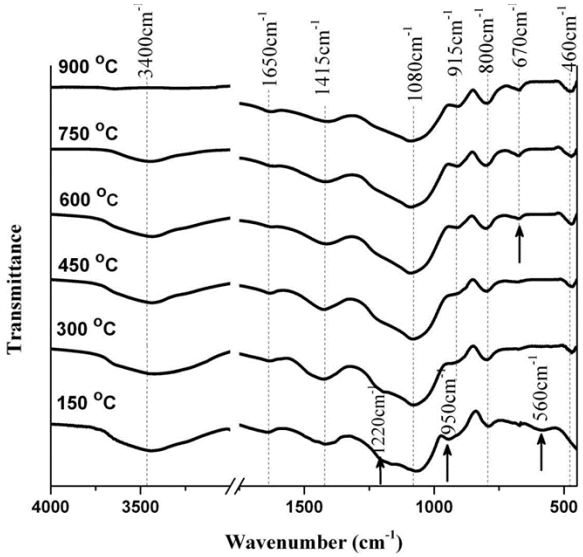

Fig. 10. IR transmittance of samples as a function of wave number after heating at different temperatures.

A principal question in the gel-glass processing is that when and how the gel converts to glass. The thermal dilatation of the synthesized compacted glass powder is shown in Fig. 11. From this figure, the glass transition temperature (T_g) and its dilatometric softening point temperature (T_d) are found to be 537 and 631°C, respectively.

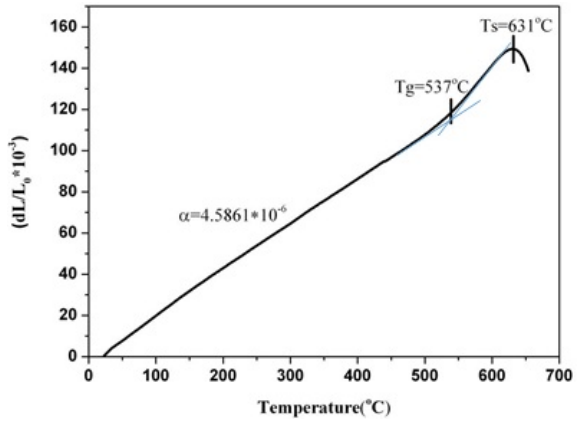

Fig. 11. Thermal dilatation of glass powder versus temperature.

According to Figs. 8-10, the weight loss of gel and formation of new B-O-Si bonds has taken place at the temperature interval of T_g - T_d. Assigning the formation of this new bond to the gel-glass conversion temperature, it can be concluded that the amorphous gel starts to convert to glassy state at approximately 600°C during heat treatment.

Fig. 12 indicates typical shrinkage variation versus temperature at the heating from 10 to 25°C/min. Several interesting features can be extracted from dilatometry curve. First, the onset temperature of sintering increases with the increase of heating rate. Second, for a given firing temperature, a smaller shrinkage is always observed at higher heating rate. Furthermore, the amount of shrinkage at different heating rates is close to each other and about 35%.

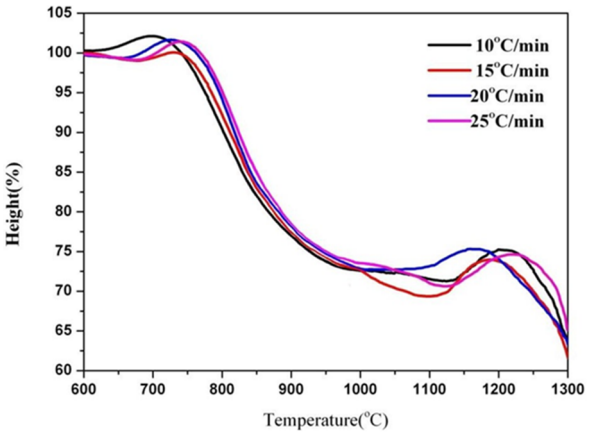

Fig. 12. Sintering curve in non-isothermal condition.

On the basis of equation (2-1) and the data shown in Fig. 12, $Ln(v/Tx^2)$ was plotted as a function of $1/T_X$ as illustrated in Fig. 13.

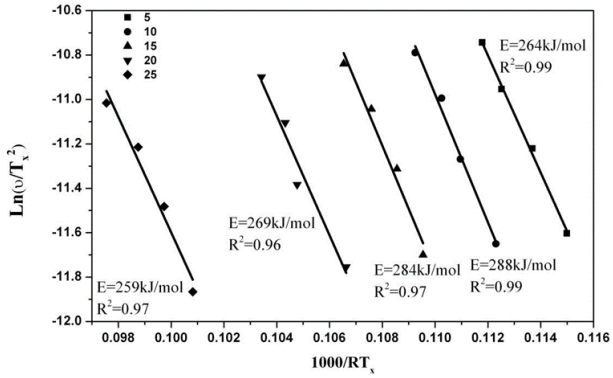

Fig. 13. Activation energy of sintering at various shrinkages.

The slops of the graphs corresponds to the sintering activation energy of 264, 288, 284, 269

[DOI: 10.22068/ijmse.2297]

and 259 kJ/mol calculated for 5, 10, 15, 20 and 25% shrinkage, accordingly. The average calculated sintering activation energy is equal to 272.8 kJ/mol.

According to fig.13, the sintering activation energy at different shrinkages values are almost similar. On the other words, in this glass, the amount of sintering activation energy does not depend on the amount of shrinkage.

4. CONCLUSIONS

Three different gel drying methods were successfully utilized to prepare monolithic crack-free glasses. Drying time was reduced from two months to about 10 and 5 h, when air drying process was replaced by IR irradiation and super critical drying methods. While dense and transparent glasses were obtained by drying the gel at the ambient pressure conditions, the specimen dried under super critical condition was porous and opaque even after sintering at 1100°C for 2 h. These observations were attributed to the high initial total pore volume and a larger mean pore size of the latter dried gel. It was concluded that the gel converted to glass during heat treatment at about 600°C, which was confirmed by evident trends of weight loss and linear shrinkage versus temperature, formation of Si-O-B bonds in the FTIR spectra as well as glass transition temperature of the specimen. While the bulk density and micro-hardness of glasses were increased by heat treatment, the super critical dried specimen showed lower bulk density and micro-hardness due to its significant residual pores.

REFERENCES

[1] E. P. R. C.J.Brinker, G.W.Scherer, "Sol-Gel-Glass: physical and structural evolution during constant heating rate experiments", Journal of Non-Crystalline Solids, vol. 72, 345–368, 1985.

[2] C. J. Brinker, S. P. Mukherjee, "Conversion of monolithic gels to glasses in a multicomponent silicate glass system", J. Mater. Sci., 16 (7), 1981, 1980–1988.

[3] L Klein, M Aparicio, A Jitianun, Handbook of Sol-Gel Science and Technology, Springer, 2018, 1-22.

[4] MA Aegerter, M Mennig, Sol-gel technologies for glass producers and users, Kluwer Academic Publishers, 2013, 13-47.

[5] B. L. Cushing, V. L. Kolesnichenko, C. J. O'Connor, "Recent advances in the liquid-phase synthesis of inorganic nanoparticles", Chem. Rev., 104 (6), 2004, 3893–3946.

[6] M. A. Einarsrud, "Light gels by conventional drying", Journal of Non-Crystalline Solids, 225, 1998, 1-7.

[7] C.A.García-González, M.C.Camino-Rey, M.Alnaief, C.Zetzl, l.Smirnova, "Supercritical drying of aerogels using CO_2: Effect of extraction time on the end material textural properties", The Journal of Supercritical Fluids, Volume 66, June 2012, 297-306.

[8] F. Kirbir, H. Murata, D. Meyers, S. Ray Chaudhuri, "Drying of aerogels in diffrent solvents between atmospheric and super critical pressure"s, Journal of Non-Crystalline Solids, 225, 1998, 14-18.

[9] QiTang, TaoWang, "Preparation of silica aerogel from rice hull ash by supercritical carbon dioxide drying, The Journal of Supercritical Fluids", Volume 35, Issue 1, August 2005, 91-94.

[10] R. Fu, B. Zheng, J. Liu, M.S. Dresselhaus, G. Dresselhaus, J.H. Satcher Jr., T.F. Baumann, "The Fabrication and Characterization of Carbon Aerogels by Gelation and Supercritical Drying in Isopropanol", Advanced Functional Materials, Volume13, Issue 7, July, 2003, 558-562.

[11] F. Shi, L. Wang, J. Liu, "Synthesis and characterization of silica aerogels by a novel fast ambient pressure drying process", J. Mater. Letters, 60 (29-30), 2006, 3718-3722.

[12] C. J. Lee, G. S. Kim, S. H. Hyun, "Synthesis of silica aerogels from water glass via new modified ambient drying", J. Mater. Sci., 37 (11), 2002, 2237-2241.

[13] S. W. Hwang, H. H. Jung, S. H. Hyun, Y. S. Ahn, "Effective preparation of crack-free silica aerogels via ambient drying", J. Sol-Gel. Science. Techn, 41 (2), 2007, 139–146.

[14] Antônio M. Barbosa Neto , Luanda G. Marques , Manoel M. Prado, Dermeval J. M. Sartori, "Mass Transfer in Infrared Drying of Gel-Coated Seeds", Advances in

[DOI: 10.22068/ijmse.2297]

Chemical Engineering and Science, 2014, 4, 39-48.

[15] D. Nowak, P. P. Lewicki, "Infrared drying of apple slices", Innovative Food Science and Emerging Technologies, 5 (3), 2004, 353-360.

[16] I. Strawbridge, P. F. James, Glass formation from gel, High performance glasses, edited by M. Cadle, J. M. Parker, Chapman and Hall, 1992. 21-62

[17] S. Ahmadi, B. Eftekhari Yekta, H. sarpoolaky, A. Aghaei, "Preparation of monolithic oxynitride glasses by sol–gel method", Journal of Non-Crystalline Solids, 404, 2014, 61–66

[18] A. Karamanov, B. Dzhantov, M. Paganelli, D. Sighinolfi, "Glass transition temperature and activation energy of sintering by optical dilatometry", Thermochim. Acta., 553, 2013, 1-7

[19] H.M. Ghartavol, M.R. Mohammadi, A. Afshara, Y. Li, "On the assessment of incorporation of CNT-TiO_2 core-shell structures into nanoparticle TiO_2 photoanodes in dye-sensitized solar cell"s, Photochemical & Photobiological Sciences, 2019, 1-31

[20] F. He, H. Zhao, X. Qu, C. Zhang, W. Qiu, "Modified aging process for silica aerogel", J. Mater.Process. Tech., 209 (3), (2009), 1621–1626.

[21] L. Stoch, M. Sroda, "Infrared spectroscopy in the investigation of oxide glass structure", J. Mol.Struct. 511-512, 1999, 77-87.

[22] M. Wang, R. Zuo, J. Jin, Sh. Su, J. Zhai, "Investigation of the structure evolution process in sol-gel derived CaO-B_2O_3-SiO_2 glass-ceramics", Journal of Non-Crystalline Solids, 357 (3), 2011, 1160-1163.

[DOI: 10.22068/ijmse.2297]